Decision Analytics Journal 9 (2023) 100355

Contents lists available at ScienceDirect

Decision Analytics Journal

journal homepage: www.elsevier.com/locate/dajour

An improved artificial rabbits optimization for accurate and efficient infinite impulse response system identification

Rizk M. Rizk-Allah [a], Serdar Ekinci [b], Davut Izci [b,*]

[a] Basic Engineering Science Department, Faculty of Engineering, Menoufia University, Shebin El-Kom 32511, Egypt
[b] Department of Computer Engineering, Batman University, Batman, 72100, Turkey

ARTICLE INFO

Keywords:
Artificial rabbits optimization
Infinite impulse response
System identification
Adaptive local search mechanism
Experience-based perturbed learning strategy

ABSTRACT

Identifying models with Infinite Impulse Response (IIR) is crucial in signal processing and system identification. This paper addresses the challenges of IIR model identification by proposing an improved version of the Artificial Rabbits Optimization (ARO) algorithm called improved ARO (IARO). The IARO algorithm integrates an adaptive local search mechanism and an experience-based perturbed learning strategy as two key enhancements to improve the effectiveness of ARO. These additions aim to address the loss of accuracy during iterations and improve the algorithm's ability to exploit promising areas. Four benchmark examples of different IIR plants are considered, and the performance of the proposed IARO algorithm is compared to existing competitive methods. The results consistently demonstrate that IARO outperforms ARO in accuracy and convergence for system identification across all orders of IIR systems. Visual analysis, convergence curves, coefficient comparison, and statistical metrics comparison all validate the superiority of the IARO algorithm. Additionally, the Wilcoxon signed-rank test results provide further statistical evidence supporting the superior performance of IARO. The comprehensive analysis showcases the efficacy and effectiveness of the IARO algorithm in accurately identifying IIR systems. This work represents a significant advancement in IIR system identification, offering a superior methodology for accurate and efficient system modeling.

1. Introduction

Identifying models with infinite impulse response (IIR) is crucial in signal processing and system identification. IIR models are commonly used to represent systems that have long-term memory, such as filters and control systems. They offer a concise representation and efficient computational solutions [1–5]. However, the identification of IIR models can be challenging due to their inherent characteristics, necessitating specialized techniques like maximum likelihood or subspace identification [6,7]. Accurate identification of IIR models is vital for the design and optimization of systems relying on them, such as digital signal processing and control systems [8–11]. Moreover, it enhances the understanding and analysis of complex systems, facilitating more effective and efficient decision-making.

In the literature, various metaheuristic algorithms have been proposed to tackle the problem of IIR system identification [12–16] due to greater ability of such algorithms to achieve near-global optimum solutions both linear and non-linear plants [17–22]. For instance, researchers have explored the application of gravitational search algorithm, inclined planes system optimization, genetic algorithm and particle swarm optimization for the design and optimization of digital IIR filters [23]. The performance and efficiency of these methods have been evaluated using mean squared error (MSE), demonstrating the successful achievement of accurate results. In a recent study [24], an enhanced version of the golden jackal optimization method was proposed, incorporating the elite opposition-based learning technique and the simplex technique, to address system identification problems, demonstrating superior efficiency, accuracy, convergence rate, precision, control parameters, and fitness value compared to other optimization algorithms. In another study [25], a modified version of the whale optimization algorithm was proposed to address the limitations of the original algorithm. By integrating opposition-based learning, exponentially decreasing function, and elite-guided Cauchy mutation, the proposed algorithm enhances exploration performance, avoids local optima, and improves solution quality and convergence rate, as demonstrated through experiments on various benchmark functions and IIR system identification tasks, outperforming seven commonly used algorithms. A different modified whale optimization algorithm has also been reported in another study for IIR identification [26]. In [27], an average differential evolution with local search was introduced for identifying optimal coefficients of unknown IIR systems.

* Corresponding author.
E-mail addresses: rizk_masoud@yahoo.com (R.M. Rizk-Allah), serdar.ekinci@batman.edu.tr, ekinciser@yahoo.com (S. Ekinci), davut.izci@batman.edu.tr, davutizci@gmail.com (D. Izci).

https://doi.org/10.1016/j.dajour.2023.100355
Received 5 August 2023; Received in revised form 5 October 2023; Accepted 31 October 2023
Available online 3 November 2023
2772-6622/© 2023 The Author(s). Published by Elsevier Inc. This is an open access article under the CC BY-NC-ND license (http://creativecommons.org/licenses/by-nc-nd/4.0/).

It is feasible to list more studies in this regard as several other metaheuristic approaches have been reported for the IIR system identification problem, such as cuckoo search algorithm [28] and it modified version [29], hybrid chimp-cuckoo algorithm [30], a sigmoid attractiveness based improved firefly algorithm [31], an enhanced slime mould algorithm [32], teacher learner-based optimization [33], grey wolf optimizer with ranking-based mutation operator [34], modified-interior search algorithm with Lèvy flight [35], firefly algorithm [36], hybrid cellular particle swarm optimization and differential evolution [37], seeker optimization algorithm [38], artificial bee colony algorithm [39], a modified version of particle swarm optimization and artificial bee colony algorithms [40,41], quantum particle swarm optimization and artificial bee colony algorithm [42]. These examples demonstrate the feasibility of employing various metaheuristic techniques to address the challenges of IIR system identification.

In the ever-continued scape of signal processing and system identification, the quest for efficient and accurate methodologies continues to drive researchers towards new innovations [43]. With an insatiable appetite for cutting-edge solutions, researchers and practitioners seek novel approaches to tackle the challenges inherent in IIR system identification. Traditional methods, while effective to a certain extent, are often plagued by limitations such as slow convergence, sensitivity to initial conditions, and suboptimal performance. Recognizing these drawbacks, the research community has been eagerly awaiting new methods that can transcend the boundaries of existing techniques and unlock new possibilities. In this pursuit, the development of intelligent algorithms has played a pivotal role in unraveling complex patterns and uncovering hidden insights within intricate systems [44–50]. In line with this motivation, this work proposes a new optimizer by improving the performance of one of the recent metaheuristic algorithms known as artificial rabbits optimization (ARO) algorithm [51].

The ARO algorithm offers simplicity in implementation and fast convergence to good solutions by identifying the best participants within the search region. However, the algorithm suffers from significant flaws that hinder its ability to handle complex and multimodal problems while striking a balance between exploration and exploitation. One major issue is that the rabbits in ARO perform the iterative process by randomly selecting a burrow, which can accelerate convergence but may degrade solution diversity and trap the rabbits in local optima. Furthermore, ARO lacks a guidance strategy to navigate towards promising regions during the iterative search, leading to potential degradation in the quality of the final solution. Overcoming this challenge of ensuring the new population reaches prospective areas presents an excellent opportunity for improvement. In essence, there is a need to enhance the effectiveness of the traditional ARO algorithm. To address these shortcomings, this paper proposes an improved version called IARO, which integrates an adaptive local search (ALS) mechanism and an experience-based perturbed learning (EPL) strategy.

Four benchmark examples of different IIR plants, along with their corresponding same and reduced order IIR filter models. The examples range from second order systems to fifth order systems, and each is evaluated using both the original form of the ARO algorithm [51] and the proposed IARO algorithm to identify the coefficients of the reduced and same orders digital IIR filters in order to estimate the unknown plants. The objective of this article is to showcase the remarkable capabilities of IARO in comparison to existing approaches.

By conducting a comprehensive empirical evaluation and performance analysis, we aim to demonstrate the superior effectiveness and efficiency of IARO in identifying IIR systems. In this context, coevolution particle swarm optimization with multi-strategy [52], differential evolution [52], differential evolution with a hybrid mutation operator and self-adapting control parameters [52], and opposition-based hybrid coral reefs optimization algorithm [52] are considered as different existing competitive methods for the second-order system modeled with reduced and same order IIR filters. For the third-order system modeled with reduced and same order IIR filters, different methods, including cat swarm optimization [53], firefly algorithm [54], hybrid particle swarm optimization and gravitational search algorithm [54], and selfish herd optimization algorithm based on chaotic strategy [54] are considered as different existing competitive methods. Similarly, for the fourth-order system modeled with reduced and same order IIR filters, bat algorithm [55], Lévy flight trajectory-based whale optimization algorithm [55], grey wolf optimizer with ranking-based mutation operator [55], and dynamic opposite learning enhanced artificial ecosystem optimizer [55] are considered as reported methods. Lastly, for the fifth-order system modeled with reduced and same order IIR filters, genetic algorithm [23], gravitational search algorithm [23], inclined planes system optimization [23], and particle swarm optimization [23] are considered.

The results consistently indicate that the IARO algorithm surpasses the conventional ARO algorithm in terms of accuracy and convergence for system identification. Regardless of the order of IIR systems, IARO consistently achieves lower MSE values, demonstrating its superior ability to minimize the discrepancy between estimated and actual system outputs. Visual analysis of scatter plots reveals a consistent pattern across all orders of IIR systems, with IARO generating data points predominantly lower than those obtained through ARO. This suggests that the IARO algorithm effectively finds optimal solutions that closely match the actual system behavior. Convergence curves further confirm this trend, as IARO consistently converges to lower MSE values compared to ARO, showcasing its superior ability to explore the search space efficiently and identify optimal solutions. The analysis of coefficient comparison supports the effectiveness of the IARO algorithm in optimizing system parameters. In all cases, the coefficients obtained through IARO exhibit closer values to the real values compared to ARO, indicating its superior ability to fine-tune system parameters and improve system identification accuracy. Furthermore, statistical metrics comparison validates the superiority of the IARO algorithm. Across all orders of IIR systems, IARO consistently achieves the best values for metrics such as best, worst, mean, and standard deviation. The best values obtained through IARO are significantly closer to the real values than those obtained through ARO and other alternative methods, highlighting the algorithm's consistent generation of solutions with superior performance and accuracy. Additionally, the Wilcoxon signed-rank test results further supports the superior performance of IARO. In summary, the comprehensive analysis of the IARO algorithm for IIR system identification demonstrates its efficacy and superiority over the conventional ARO algorithm and other existing methods as it consistently achieves lower MSE values, better convergence, optimized system coefficients, and superior statistical metrics. These findings underscore IARO's ability to effectively explore the search space, identify optimal solutions, and accurately model underlying IIR systems. Therefore, IARO algorithm represents a significant advancement in the pursuit of superior effectiveness in IIR system identification.

The contributions and novelty of this work lie in the introduction of the IARO algorithm, its enhancements over ARO, the integration of novel strategies (ALS and EPL), and its superior performance demonstrated through comprehensive empirical evaluation and benchmarking against existing optimization methods in the context of IIR system identification. In line with the discussion so far, the novelty of this work and the contributions can briefly be highlighted as follows.

(1) This work introduces the IARO algorithm, addressing the limitations of existing optimization methods for IIR system identification.
(2) IARO introduces significant enhancements to the traditional ARO algorithm, making it more effective in solving complex problems, which is a novel contribution to the field of system identification.
(3) IARO integrates an ALS mechanism and an EPL strategy to enhance its performance, offering a unique approach to optimization. The integration of those mechanisms within IARO represents a novel approach that improves its ability to navigate complex search spaces.

(4) The study conducts a comprehensive empirical evaluation, comparing IARO with a wide range of competitive optimization algorithms, including particle swarm optimization, genetic algorithms, and various hybrid methods. The extensive benchmarking of IARO against a diverse set of competitive algorithms in IIR system identification is a novel aspect, demonstrating its effectiveness and superiority across various scenarios.
(5) Results consistently show that IARO outperforms ARO and other existing methods in terms of accuracy, convergence, and the ability to identify optimal solutions for IIR system identification. IARO consistently achieves lower MSE values, better convergence, and optimized system coefficients, showcasing its consistent and superior performance compared to existing methods.
(6) The validation of statistical metrics further highlights the novelty of IARO in consistently generating superior solutions for system identification.

The remaining sections of the paper are organized as follows: Section 2 provides a brief explanation of the ARO algorithm and its mathematical structure. Section 3 explains the proposed IARO algorithm. Section 4 presents the details regarding IIR system identification and the design procedure using digital IIR filtering systems to accurately represent unknown plants. The subsequent section presents simulation results obtained for different benchmark examples and discusses the significance of the IARO-based design method compared to other state-of-the-art existing methods. Finally, the paper concludes in Section 6.

2. The conception of artificial rabbits optimization

The artificial rabbits optimization (ARO) algorithm is a recent and potent metaheuristic technique inspired by the survival natures of rabbits [51], such as random hiding and detour foraging. The foraging mode of the ARO is modeled mathematically to perform the iterative searches. In this sense, A rabbit attempts to eat the plants and grasses adjacent to other rabbits' burrows. This action might aid in fooling predators and defending the rabbit burrow from attacks. In other words, rabbits ignore the food that is readily available nearby and instead look for food in faraway locations. The ARO algorithm uses the number of rabbits as the swarm population. Each rabbit has an eating zone with some grass and plants in addition to a d burrows. Each rabbit randomly visits the burrows of other rabbits in search of food. Each rabbit tends to update its current location with respect to the randomly chosen individual and contributes a disruption throughout this stage. This foraging action can be represented mathematically as follows [51]:

$$\vec{\Delta}_i(t+1) = \vec{z}_j(t) + \rho.\left(\vec{z}_i(t) - \vec{z}_j(t)\right) + round\left(0.5.\left(0.05 + g_1\right)\right).n_1, i, j = 1, 2 \ldots \ldots, M \text{ and } i \neq j \quad (1)$$

$$\rho = E.c \quad (2)$$

$$E = \left(e - e^{\left(\frac{1-t}{T}\right)^2}\right).\sin(2\pi g_2) \quad (3)$$

$$c(k) = \begin{cases} 1 & \text{if } k == h(u) \\ 0 & else \end{cases}, k = 1, \ldots, d \,\&\, u = 1, 2, \ldots, \lceil g_3.d \rceil \quad (4)$$

$$h = randperm(d) \quad (5)$$

$$n_1 \sim N(0, 1) \quad (6)$$

where $\vec{z}_i(t), \vec{\Delta}_i(t+1), M, T, d, round, randperm$, and E define the current position of candidate of ith candidate at time t, ith updated candidate at time $t+1$, population size of rabbits, the total size of iterations, the problem dimension, the rounding to the nearest integer value, random permutation function ranged from 1 to problem dimension, and running length during foraging, respectively. Here n_1 denotes normal distribution function, and g_1, g_2, g_3 define uniform random numbers inside the interval [0, 1]. ARO is assisted by the perturbation in Eq. (6) to avoid local maxima/minima and carry out a comprehensive search. The running distance (E) helps in conducting longer distances during the early iterations and shorter distances in the later iterations to perform the exploration and exploitation modes, respectively. Here ρ represents a mathematical operator that simulates the locomotion of rabbits, and c is a vector that is used in the search process to select a number of individuals. Therefore, this foraging stage boosts the ARO algorithm's exploration and global search capabilities. In the exploitation mode, rabbits randomly hide to avoid being caught by predators. In close proximity to its burrows, the rabbit creates a few burrows. During each iteration of ARO, a rabbit consistently creates b burrows throughout each dimension and it chooses a burrow at random and hides there to fool the predators.

The ith rabbit with jth burrow can be formulated as follows [51]:

$$\vec{BU}_{ij}(t) = \vec{z}_i(t) + H.h.\vec{z}_i(t), i = 1, 2 \ldots \ldots, M \text{ and } j = 1, 2 \ldots \ldots, d \quad (7)$$

$$H = \frac{1 - t + T}{T} g_4 \quad (8)$$

$$n_2 \sim N(0, 1) \quad (9)$$

$$h(k) = \begin{cases} 1 & \text{if } k == j \\ 0 & else \end{cases}, k = 1, \ldots, d \quad (10)$$

where H and d denote the hiding function, and formed burrows within the area of the rabbit, respectively. Primarily, a bunny's big area is where holes are generated. The size of this neighborhood shrinks as the amount of iterations rises. the random hiding mode is offered as follows [51].

$$\vec{\Delta}_i(t+1) = \vec{z}_i(t) + \rho.\left(g_4.BU_{ir}(t) - \vec{z}_i(t)\right), i = 1, 2, \ldots \ldots M \quad (11)$$

$$h_r(k) = \begin{cases} 1 & \text{if } k == \lceil g_5.d \rceil \\ 0 & else \end{cases}, k = 1, \ldots, d \quad (12)$$

$$BU_{ir}(t) = \vec{z}_i(t) + H.h_r.\vec{z}_i(t) \quad (13)$$

where $BU_{ir}(t)$ denotes the chosen burrow by the rabbit through the hiding mode, g_4 and g_5 define random numbers inside the interval [0, 1]. The ith rabbit's position is updated after either a detour foraging mode or a random hiding process as follows [51].

$$\vec{z}_s(t+1) = \begin{cases} \vec{z}_s(t) & f(\vec{z}_s(t)) \leq f(\vec{\Delta}_s(t+1)) \\ \vec{\Delta}_s(t+1) & f(\vec{z}_s(t)) > f(\vec{\Delta}_s(t+1)) \end{cases} \quad (14)$$

If the sth rabbit's candidate fitness is better than the position's present fitness, the bunny leaves its current location and stays in the candidate location determined by either Eq. (1) or Eq. (11). The energy of rabbits is shrinking with the progress of iteration, which helps in the transition from explorative mode to exploitative mode, which is formulated as follows [51]:

$$EA(t) = 4\left(1 - \frac{t}{T}\right)\ln\left(\frac{1}{\alpha}\right) \quad (15)$$

where α defines a random number. When $EA(t) > 1$, the algorithm searches globally for the solution (exploration); when $EA(t) \leq 1$, the algorithm searches locally for the solution (exploitation). The pseudo-code framework of the original ARO is presented in Fig. 1.

3. The proposed IARO algorithm

ARO can obtain the best participants in the search region with the advantages of its simplicity in implementation and the fast convergence to good solutions by estimating its development. The algorithm still has significant flaws, though, that could lead to signation dilemmas and prevent it from finding a balance between exploitative and exploratory patterns when it comes to handling multimodal and complex issues. Firstly, the rabbits perform the iterative process by choosing a burrow at random; although this scheme can accelerate the convergence pattern, the solution diversity may degrade, leading to the rabbits getting stuck in the local optimal solution. Firstly, no guidance strategy is

```
Initialize a set of rabbits randomly
Evaluate the fitness of each rabbit and determine the best one (z_best)
While the stopping criterion not met do
  for i = 1 : M
  Compute the energy of rabbit (EA) by Eq. (15)
    if EA > 1
      Select a rabbit randomly from the population
      Obtain ρ by Eqs. (2)-(6)
      Carry out the detour foraging phase by Eq. (1)
      Evaluate the fitness of the rabbit
      Update the rabbit' position by Eq. (14)
    else
      Create d burrows and elicit one of them randomly as hiding position by Eq. (13)
      Conduct random hiding by Eq. (11)
      Evaluate the fitness of the rabbit
      Update the rabbit' position by Eq. (14)
    End if
    Update the best so far solution (z_best)
  End for
End while
Output: Return z_best
```

Fig. 1. The framework of the ARO.

employed in the ARO to approach the promising regions during the iterative search, which may deteriorate the quality of the final solution. Therefore, figuring out how to make sure that the new population can get to the prospective area is a good challenge. In other words, there are opportunities to improve the effectiveness of the traditional ARO. Hence, an improved ARO, named IARO, based on adaptive local search (ALS) mechanism, and experience-based perturbed learning (EPL) strategy are proposed in this paper.

3.1. The prospective of EPL strategy

In the IARO algorithm, the rabbits are behaved by following another rabbit from the population during the exploration phase. This update scheme can lead to a pattern of invasive diversification. Therefore, the EPL is embedded to discover more promising regions inside the feasible search space, thus boosting the exploration search. In particular, the EPL starts by calculating the mean (Δ^{it}_{mean}) and the deviation (Δ^{it}_{dev}) of any solution chosen randomly with respect to the best so far solution (Δ_{best}). Afterwards, the new solution is updated according the Δ^{it}_{mean} and Δ^{it}_{dev} along with perturbed term. Therefore, the updated solution can be expressed as follows.

$$\Delta^{it}_{mean} = (z_{best} + z^{it}_I)/2 \tag{16}$$

$$\Delta^{it}_{dev} = \mathrm{abs}(z_{best} - z^{it}_I) \tag{17}$$

$$\Delta^{it}_C = \Delta^{it}_{mean} + rand_1.\Delta^{it}_{dev} \tag{18}$$

$$\begin{aligned} z^{it}_{new} &= \Delta^{it}_C + rand_2.(z_{best} - \Delta^{it}_C) \\ &\quad + 0.95^{it}.(rand_3 - 0.5).\mathrm{abs}(z_{max,j} - z_{min,j}), z_{max,j} \\ &= max_j\left\{z^{it}_i\right\}, z_{min,j} = min_j\left\{z^{it}_i\right\} \forall i \end{aligned} \tag{19}$$

where Δ^{it}_I stand for any arbitrary solution chosen at random, $rand_1$, $rand_2$, and $rand_3$ define three random numbers elicited according to the uniform distribution inside the interval $[0, 1]$. Here, the third term of Eq. (19) is to perform perturbed solution within the dynamic bounders (Δ_{max} and Δ_{min}).

3.2. The prospective of ALS strategy

To mitigate the loss of accuracy during the iterative process and enhance the exploitation trend towards the promising space, an adaptive local search (ALS) strategy is purported as a guidance scheme based on shared information among the elite group within the rabbits along with their best individual (z_{best}) and worst individual (z_{worst}). To be specific, the process by determining the elite group according to the fitness function as well as identifying the worst and best individuals within this grope (z^P and z^W). Afterwards, three types of movements are adopted to perform the updating step, which are pushing z^W in the direction of z^P, or pushing z^W towards z_{best}, and pushing z^W in the direction of the average of z^P and z_{best}. These movements are carried out in sequential manner and it stops after a certain one reaches better fitness. The updating phase of this strategy can be expressed as follows:

$$z^{it+1}_I = \begin{cases} z^{\mathrm{ALS}}_1 = 2\times r_1 \times \left(z^P - z^W\right) + z^W & \text{if } f(z^{\mathrm{ALS}}_1) \le f(z^{it}_I) \\ z^{\mathrm{ALS}}_2 = 2\times r_2 \times \left(z_{best} - z^W\right) + z^W & \text{else if } f(z^{\mathrm{ALS}}_2) \le f(z^{it}_I) \\ z^{\mathrm{ALS}}_3 = 2\times r_3 \times \left(\left(z^P + z_{best}\right)/2 - z^W\right) + z^W & otherwise \end{cases} \tag{20}$$

where z^{it}_I and z^{it+1}_I stand for the present and updated solutions of the ith solution inside the elite class. The framework of the proposed IARO is represented as in Fig. 2.

4. Problem definition of IIR system identification and recommended approach

System identification involves mathematically representing an unknown system based on input and output data [56]. The goal is to minimize an error function using an optimization algorithm, which finds the best model that closely matches the actual plant's output. IIR models offer the advantage of using fewer parameters while meeting performance requirements and providing accurate representations of physical plants for real-world applications [57]. Fig. 3 illustrates the implementation of the IARO algorithm for the IIR system identification problem.

In here, $y(k)$ and $d(k)$ respectively represent the output of the IIR filter and the unknown plant. On the other hand, $x(k)$ stands for the applied input signal whereas m and n are respectively the coefficients of the numerator and denominator. From the information provided in

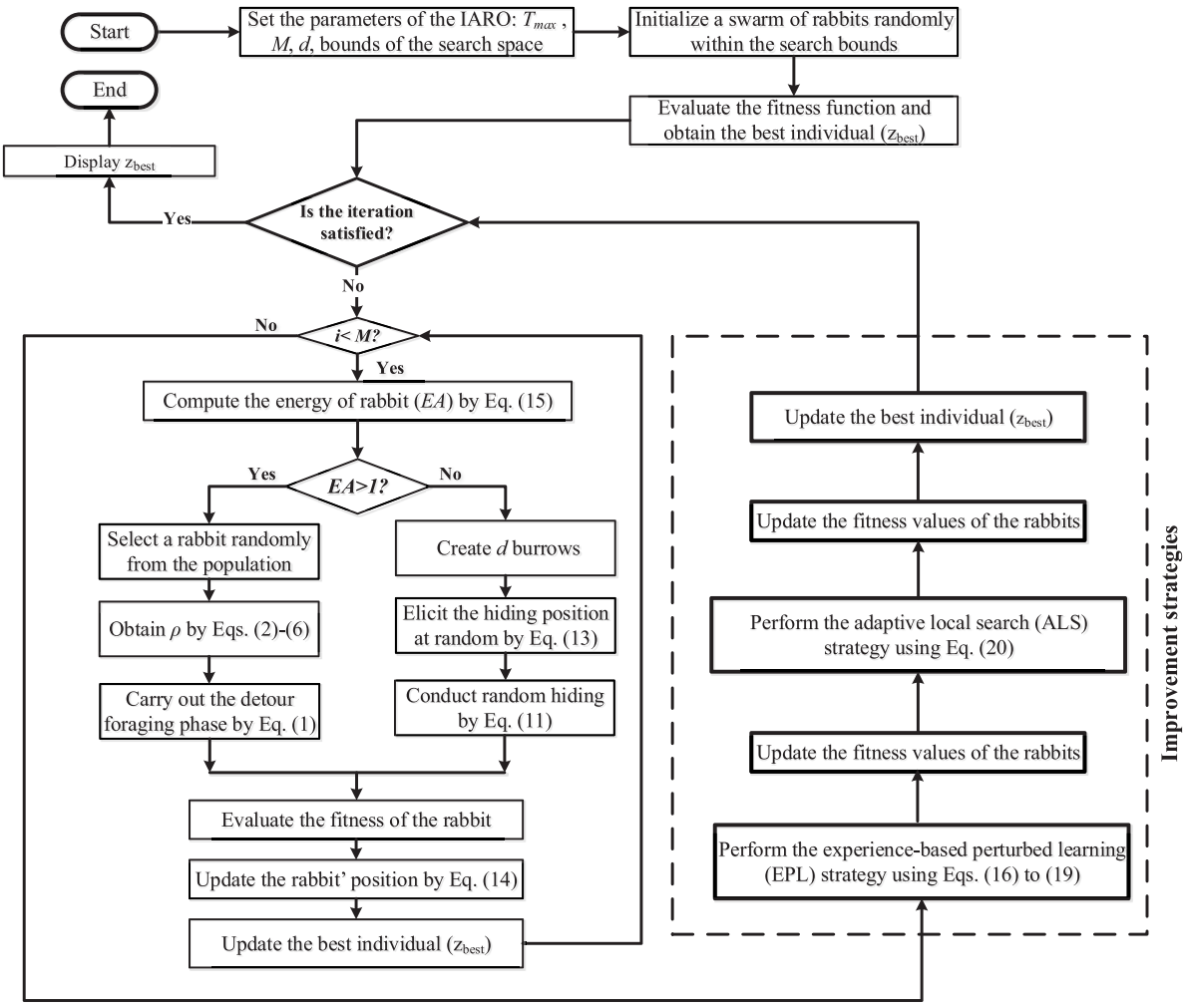


Fig. 2. The framework of the proposed IARO.

Fig. 3, the transfer function of an IIR system can be represented as follows [58].

$$\frac{Y(z)}{X(z)} = \frac{\left(b_0 + b_1 z^{-1} + b_2 z^{-2} + \cdots + b_m z^{-m}\right)}{\left(1 + a_1 z^{-1} + a_2 z^{-2} + \cdots + a_n z^{-n}\right)} \tag{21}$$

Here, the coefficients a_i and b_j denote the poles and zeros of the IIR model, where $i = 1, 2, \ldots, n$ and $j = 0, 1, \ldots, m$. The difference equation form of the latter transfer function can be written as follows [58].

$$y(k) + \sum_{i=1}^{n} a_i \cdot y(k-i) = \sum_{j=0}^{m} b_j \cdot x(k-j) \tag{22}$$

The error between the model and the actual plant (shown in Fig. 3) is represented as $e(k) = d(k) - y(k)$, where $e(k)$ serves as the objective for minimizing the identification problem. The objective function (MSE) is defined as [59]:

$$f(\theta) = MSE = \frac{1}{W} \sum_{k=1}^{W} (d(k) - y(k))^2 \tag{23}$$

where W is the number of samples used in the simulation. By adjusting the parameter vector θ, the goal is to minimize the cost function $f(\theta)$. The algorithm aims to find the optimal parameters that minimize the discrepancy between the estimated and actual system outputs, improving the accuracy and convergence of the identification process.

5. Simulation results

This study conducted simulations to analyze the performance of different IIR systems. The input to the system, denoted as $x(k)$, was generated as a uniformly distributed white sequence ranging from −0.5 to 0.5. The MSE cost function was calculated based on a data length of 200 ($W = 200$). The experiments were conducted with specific parameters for the algorithm. The algorithm was run 30 times, with a maximum number of iterations (T) set to 500, and a population size of 100 individuals (M). The implementations were carried out on MATLAB/Simulink that is installed on a windows computer with 12th Gen Intel i5-12400, 2.50 GHz processor and 16.00 GB RAM. Fig. 4 displays the input signal used in the simulations.

This signal was applied to the transfer functions of the IIR filters and their corresponding plants. Table 1 presents four benchmark examples of different IIR plants, along with their corresponding same and reduced order IIR filter models. The examples range from second order systems to fifth order systems, and each is evaluated using both the original form of the ARO algorithm [51] and the proposed IARO algorithm. The following subsections delve into the specific details of these systems and provide a comparative performance assessment of the IARO algorithm compared to the original ARO algorithm. It is worth noting that in this study, the MSE values are expressed in their raw form. For better interpretability, they can be converted to decibels

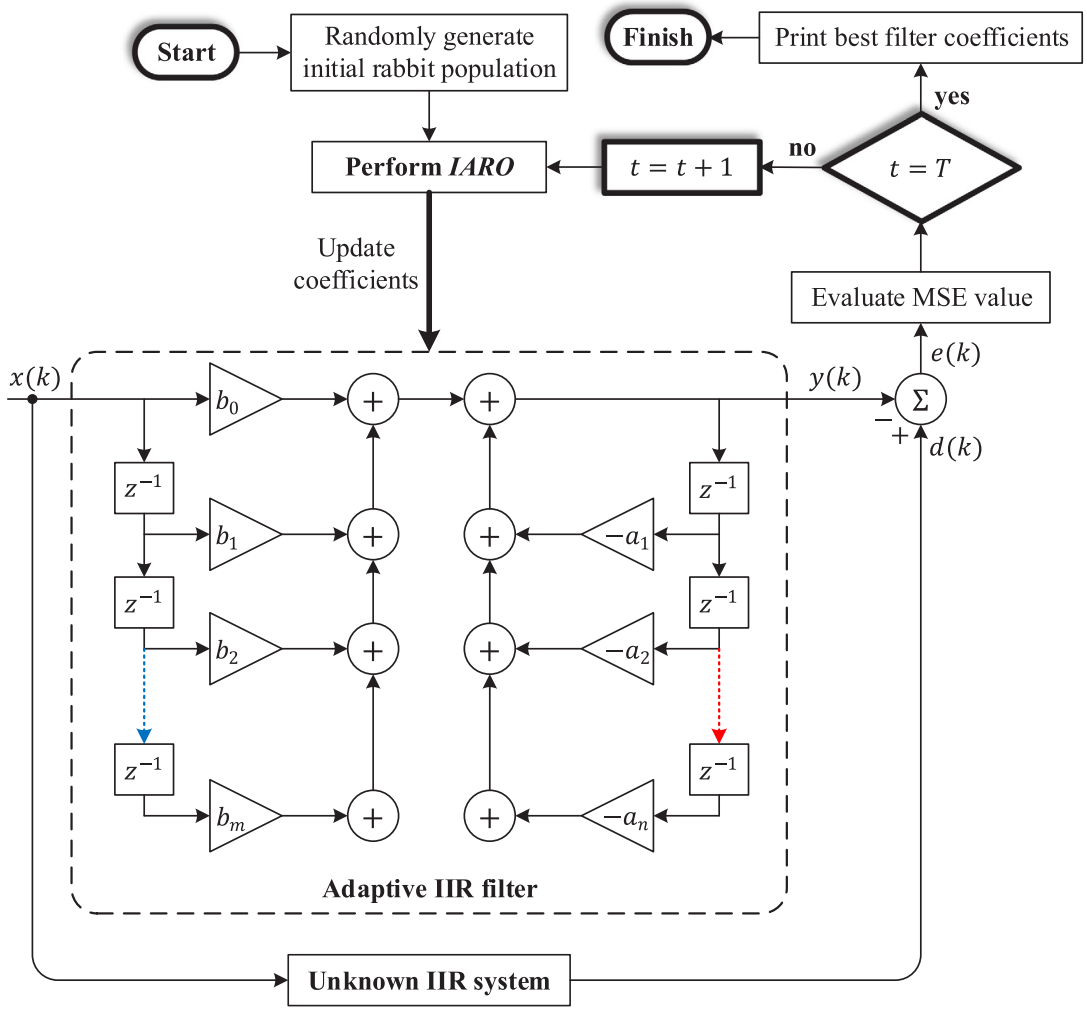


Fig. 3. Implementation of the IARO algorithm for the IIR system identification problem.

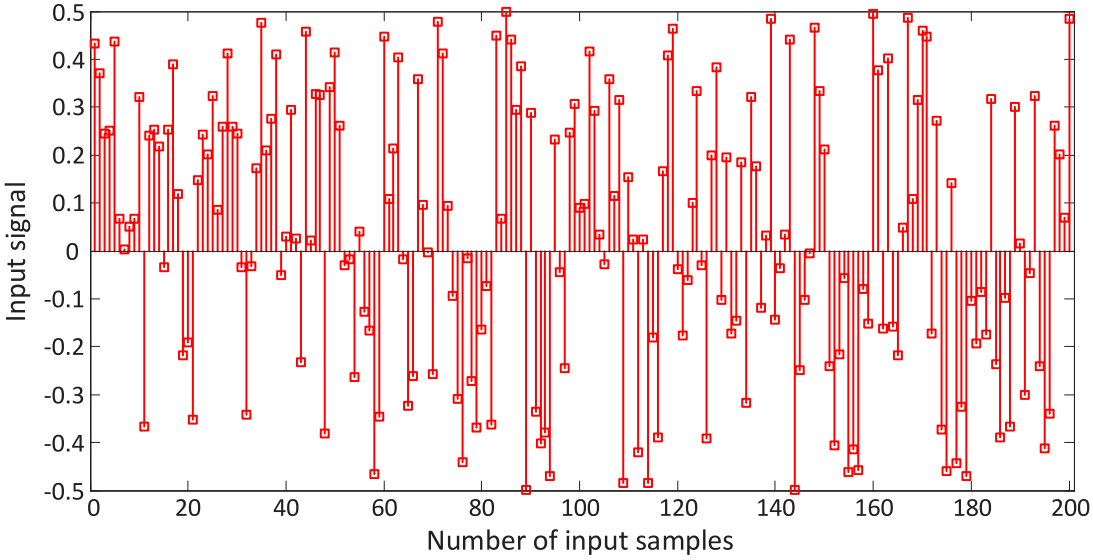


Fig. 4. The input signal used for simulations.

Table 1
Transfer functions of different IIR plants along with their representative same and reduced order IIR filter models.

System type		Transfer function of the system	Data lengths
Second order [52]	Plant ($H_p(z)$)	$\frac{0.05-0.4z^{-1}}{1-1.1314z^{-1}+0.25z^{-2}}$	$W=200$
	Same order model ($H_s(z)$)	$\frac{b_0+b_1z^{-1}}{1-a_1z^{-1}-a_2z^{-2}}$	
	Reduced order model ($H_r(z)$)	$\frac{b'_0}{1-a'_1z^{-1}}$	
Third order [53,54]	Plant ($H_p(z)$)	$\frac{-0.2-0.4z^{-1}+0.5z^{-2}}{1-0.6z^{-1}+0.25z^{-2}-0.2z^{-3}}$	$W=200$
	Same order model ($H_s(z)$)	$\frac{b_0+b_1z^{-1}+b_2z^{-2}}{1-a_1z^{-1}-a_2z^{-2}-a_3z^{-3}}$	
	Reduced order model ($H_r(z)$)	$\frac{b'_0+b'_1z^{-1}}{1-a'_1z^{-1}-a'_2z^{-2}}$	
Fourth order [55]	Plant ($H_p(z)$)	$\frac{1-0.9z^{-1}+0.81z^{-2}-0.729z^{-3}}{1+0.04z^{-1}+0.2775z^{-2}-0.2101z^{-3}+0.14z^{-4}}$	$W=200$
	Same order model ($H_s(z)$)	$\frac{b_0+b_1z^{-1}+b_2z^{-2}+b_3z^{-3}}{1-a_1z^{-1}-a_2z^{-2}-a_3z^{-3}-a_4z^{-4}}$	
	Reduced order model ($H_r(z)$)	$\frac{b'_0+b'_1z^{-1}+b'_2z^{-2}}{1-a'_1z^{-1}-a'_2z^{-2}-a'_3z^{-3}}$	
Fifth order [23]	Plant ($H_p(z)$)	$\frac{0.1084+0.5419z^{-1}+1.0837z^{-2}+1.0837z^{-3}+0.5419z^{-4}+0.1084z^{-5}}{1+0.9853z^{-1}+0.9738z^{-2}+0.3864z^{-3}+0.1112z^{-4}+0.0113z^{-5}}$	$W=200$
	Same order model ($H_s(z)$)	$\frac{b_0+b_1z^{-1}+b_2z^{-2}+b_3z^{-3}+b_4z^{-4}+b_5z^{-5}}{1-a_1z^{-1}-a_2z^{-2}-a_3z^{-3}-a_4z^{-4}-a_5z^{-5}}$	
	Reduced order model ($H_r(z)$)	$\frac{b'_0+b'_1z^{-1}+b'_2z^{-2}+b'_3z^{-3}+b'_4z^{-4}}{1-a'_1z^{-1}-a'_2z^{-2}-a'_3z^{-3}-a'_4z^{-4}}$	

(dB). The conversion from MSE to dB is achieved using the following formula:

$$MSE(\text{dB}) = 10 \cdot \log_{10}(MSE) \tag{24}$$

where $MSE(\text{dB})$ represents the MSE value in decibels.

5.1. Second order system

In this subsection, we focus on evaluating the performance of the IARO algorithm compared to the ARO algorithm and other existing approaches for a second-order system. The results, presented in Figs. 5 and 6, as well as Tables 2 and 3, provide comprehensive insights into the superiority of the IARO algorithm. Figs. 5(a) and 5(b) display the scatter plots obtained for all 30 runs of the algorithms for the second-order system modeled with same order and reduced order IIR filters, respectively. These plots visually demonstrate the performance of IARO and ARO algorithms. In Fig. 5(a), it is evident that the IARO algorithm consistently produces lower values compared to the ARO algorithm. Similarly, in Fig. 5(b), the majority of data points obtained with IARO are lower than those obtained with ARO, indicating the improved performance of IARO for both same and reduced order IIR filters. Furthermore, Fig. 6 presents the convergence curves for the second-order system, both for the case of same order (Fig. 6(a)) and reduced order (Fig. 6(b)) IIR filters. The convergence curves illustrate the progress of the algorithms over iterations. It is noteworthy that the IARO algorithm achieves lower (best) mean square error (MSE) values for both cases, indicating its effectiveness in minimizing the error and converging to better solutions.

Table 2 provides a detailed comparison of the coefficients obtained for the second-order system using the IARO and ARO algorithms. Analyzing the coefficients obtained with IARO reveals that they consistently yield closer to the real values for most parameters compared to ARO. This suggests that the IARO algorithm is capable of optimizing the system coefficients more effectively, leading to improved performance. Table 3 reports statistical values of different methods, including ARO [51], coevolution particle swarm optimization with multi-strategy (ICPSO-MS) [52], differential evolution (DE) [52], differential evolution algorithm with a hybrid mutation operator and self-adapting control parameters (HSDE) [52], and opposition-based hybrid coral reefs optimization algorithm (OHCRO) [52], for the second-order system modeled with reduced and same order IIR filters. The metrics evaluated include "best", "worst", "mean", and "standard deviation". The comparisons are performed separately for the same order system and the reduced order system.

Table 2
The coefficients obtained for second order system.

Type	Coefficients	IARO	ARO
Same order	a_1	1.131400000000000	1.131400003413515
	a_2	−0.250000000000000	−0.250000002996107
	b_0	0.050000000000000	0.050000000703819
	b_1	−0.400000000000000	−0.399999999254669
Reduced order	a'_1	0.923418356533178	0.904559639165061
	b'_0	−0.218395277719291	−0.251379456514612

Analyzing Table 3, we observe that the IARO algorithm consistently outperforms the other methods in terms of achieving the best results across all metrics. For the same order system, IARO achieves a best value of 0, significantly outperforming ARO and other methods. Similarly, for the reduced order system, IARO achieves the best values with notably lower magnitudes compared to the alternatives. Moreover, the IARO algorithm demonstrates superior performance in terms of worst, mean, and standard deviation values, indicating its robustness and stability in generating consistently better results. In summary, the evaluation of the second-order system confirms the superiority of the IARO algorithm over ARO and other existing approaches.

5.2. Third order system

In this subsection, we evaluate the performance of the IARO algorithm for a third-order system. The results, presented in Figs. 7 and 8, as well as Tables 4 and 5, provide insights into the algorithm's effectiveness in comparison to ARO and other existing approaches. Figs. 7(a) and 7(b) illustrate the scatter plots obtained for all 30 runs of the algorithms for the third-order system, considering reduced and same order IIR filters. These scatter plots exhibit a similar pattern

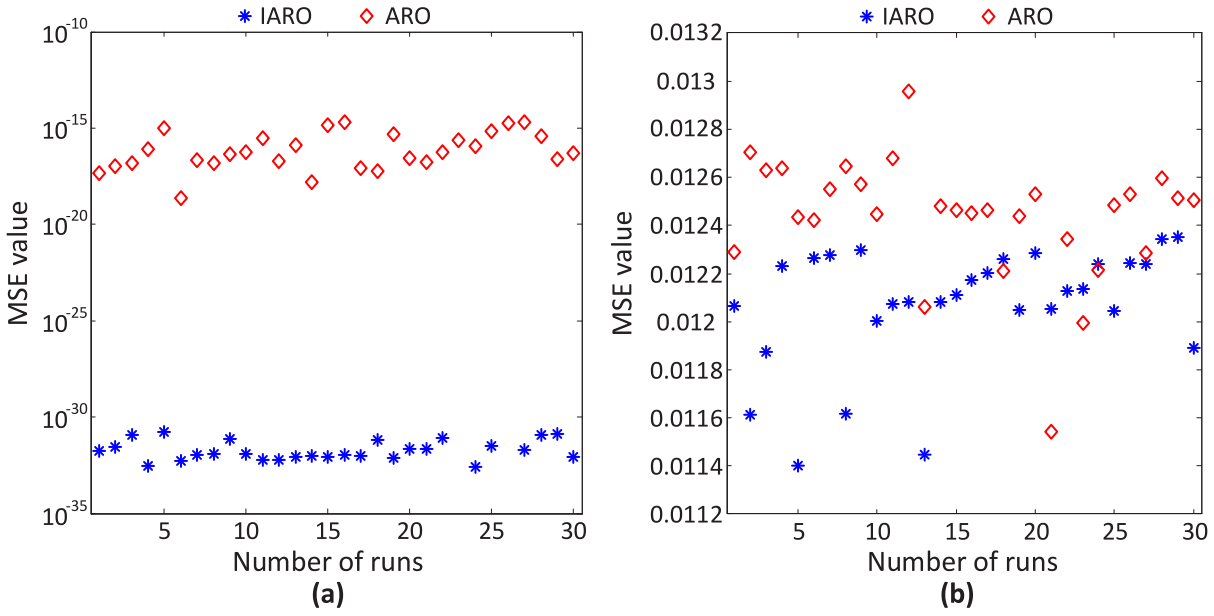


Fig. 5. Scatter plots obtained for all 30 runs of algorithms for second order system modeled with (a) same order and (b) reduced order IIR filters.

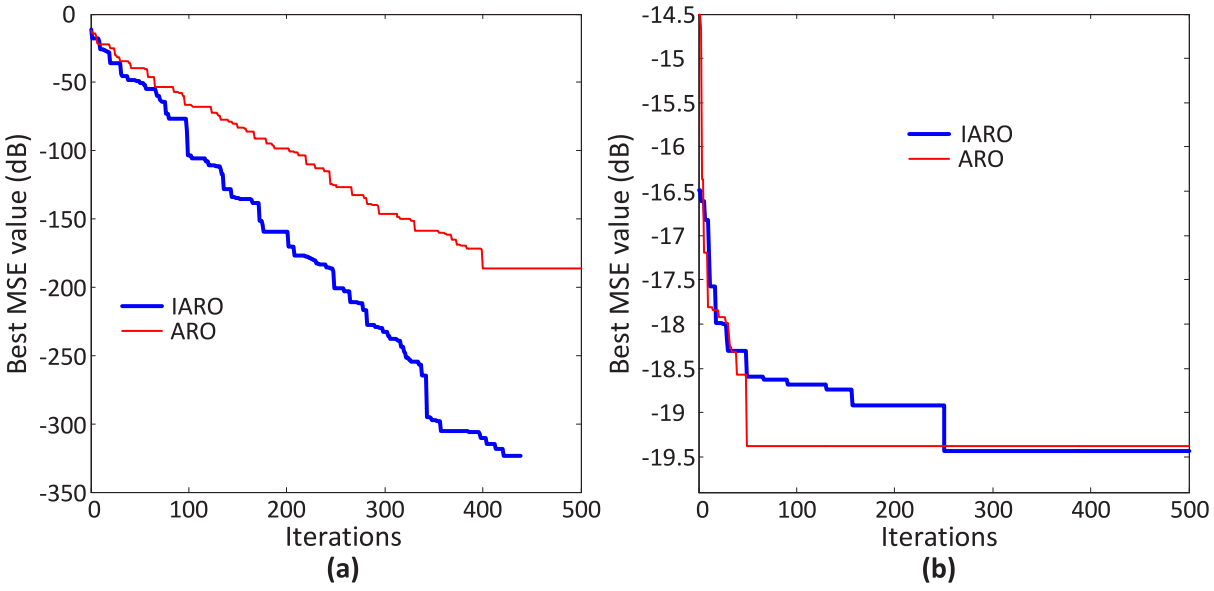


Fig. 6. Convergence curves obtained for second order system modeled with (a) same order and (b) reduced order IIR filters.

Table 3
Reported statistical values of different methods for the second order system modeled with the same and reduced order IIR filters.

Type	Metric	IARO	ARO	ICPSO-MS	DE	HSDE	OHCRO
Same order	Best	**0**	2.4432×10^{-19}	8.83×10^{-14}	9.63×10^{-10}	6.22×10^{-14}	1.93×10^{-15}
	Worst	$\mathbf{1.6120 \times 10^{-31}}$	2.0901×10^{-15}	7.79×10^{-5}	9.78×10^{-9}	2.15×10^{-8}	1.48×10^{-9}
	Mean	$\mathbf{3.3556 \times 10^{-32}}$	3.6551×10^{-16}	1.96×10^{-6}	6.36×10^{-9}	2.99×10^{-9}	7.53×10^{-11}
	Standard Deviation	$\mathbf{4.4641 \times 10^{-32}}$	6.2478×10^{-16}	1.90×10^{-6}	2.30×10^{-9}	6.18×10^{-9}	2.62×10^{-10}
Reduced order	Best	$\mathbf{1.1401 \times 10^{-2}}$	1.1542×10^{-2}	0.1359	0.1403	0.1138	0.1320
	Worst	$\mathbf{1.2351 \times 10^{-2}}$	1.2956×10^{-2}	0.1848	0.1846	0.1441	0.1954
	Mean	$\mathbf{1.2069 \times 10^{-2}}$	1.2436×10^{-2}	0.1607	0.1638	0.1302	0.1605
	Standard Deviation	$\mathbf{2.5258 \times 10^{-4}}$	2.5626×10^{-4}	0.0139	0.0131	0.00956	0.0134

to the previous case of the second-order system (Fig. 5). Specifically, in Fig. 7(a), the IARO algorithm consistently produces lower values compared to ARO. Similarly, in Fig. 7(b), the majority of data points obtained with IARO are lower than those obtained with ARO, suggesting the improved performance of IARO for both same and reduced order IIR filters. Furthermore, Fig. 8 presents the convergence curves for the third-order system, considering the same order (Fig. 8(a)) and reduced order (Fig. 8(b)) IIR filters. The convergence curves demonstrate the progress of the algorithms over iterations. Analogous to the second-order system, IARO achieves lower MSE values for both cases,

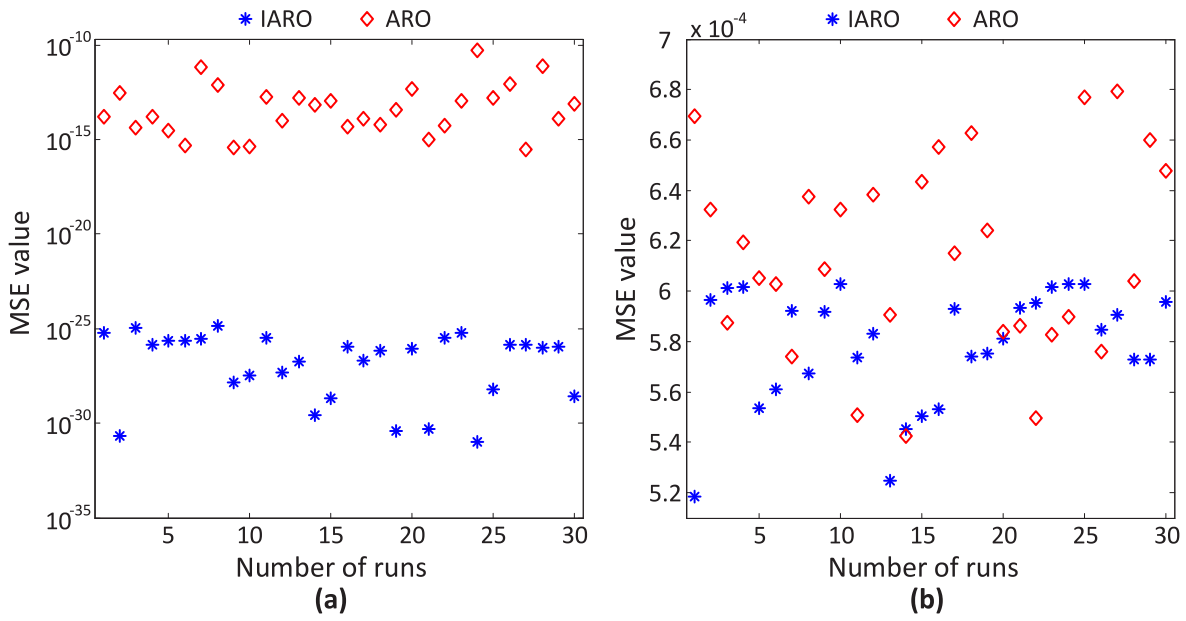


Fig. 7. Scatter plots obtained for all 30 runs of algorithms for third order system modeled with (a) same order and (b) reduced order IIR filters.

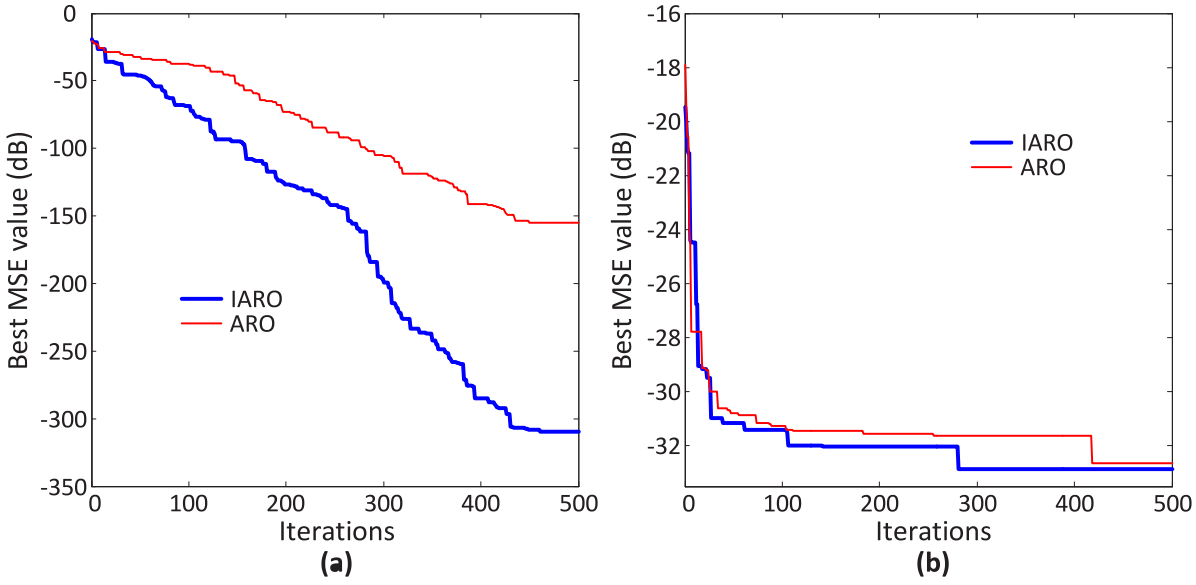


Fig. 8. Convergence curves obtained for third order system modeled with (a) same order and (b) reduced order IIR filters.

indicating its effectiveness in minimizing the error and converging to superior solutions.

Table 4 provides a detailed comparison of the coefficients obtained for the third-order system using the IARO and ARO algorithms. Analyzing the coefficients obtained with IARO reveals that they generally yield closer to the real values for most parameters compared to ARO. This indicates the IARO algorithm's ability to optimize the system coefficients effectively, leading to improved performance. Table 5 reports the statistical values of different methods, including ARO [51], cat swarm optimization (CSO) [53], firefly algorithm (FFA) [54], hybrid particle swarm optimization and gravitational search algorithm (HPSO-GSA) [54], and selfish herd optimization algorithm based on chaotic strategy (CSHO) [54], for the third-order system modeled with reduced and same order IIR filters. The statistical metrics are evaluated separately for the same order and reduced order cases.

Examining Table 5, we observe that the IARO algorithm consistently outperforms the other methods in terms of the best values across all metrics. For the same order system, IARO achieves a best value of 9.8757E−32, outperforming ARO and other methods. Similarly, for the reduced order system, IARO attains the best values with significantly lower magnitudes compared to the alternatives. Additionally, the IARO algorithm exhibits favorable performance in terms of worst, mean, and standard deviation values, indicating its robustness and stability in generating consistently better results.

In summary, the evaluation of the third-order system demonstrates the superiority of the IARO algorithm over ARO and other existing approaches. The analysis of scatter plots, convergence curves, coefficient comparison, and statistical metrics consistently highlight the improved performance of IARO in terms of achieving lower MSE, better convergence, optimized coefficients, and superior statistical values.

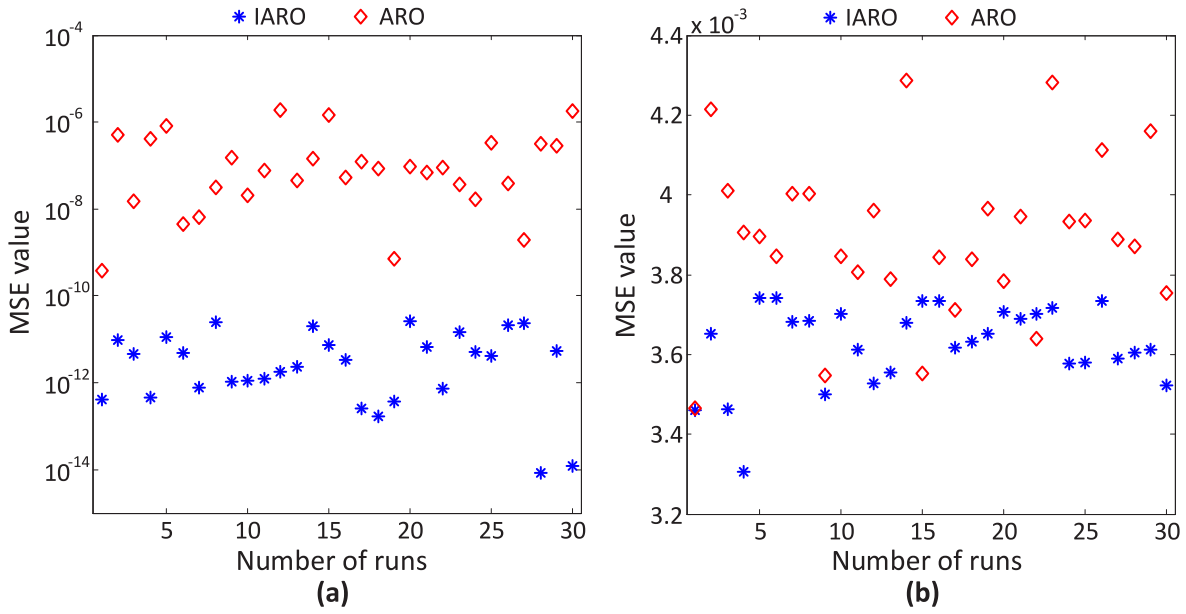


Fig. 9. Scatter plots obtained for all 30 runs of algorithms for fourth order system modeled with (a) same order and (b) reduced order IIR filters.

Table 4
The coefficients obtained for third order system.

Type	Coefficients	IARO	ARO
Same order	a_1	0.599999999999999	0.599999875820786
	a_2	−0.250000000000001	−0.250000068017135
	a_3	0.199999999999999	0.199999912346179
	b_0	−0.199999999999999	−0.200000033539383
	b_1	−0.400000000000000	−0.400000015678280
	b_2	0.499999999999999	0.499999915612248
Reduced order	a_1'	−0.150804672088005	−0.172640146509279
	a_2'	−0.363071095485534	−0.382015500260903
	b_0'	−0.212213933861540	−0.208604004333586
	b_1'	−0.593635989853768	−0.582547136297091

These findings establish the effectiveness and superiority of the IARO algorithm for the considered third-order system.

5.3. Fourth order system

In this section, we examine the performance of the IARO algorithm for a fourth-order system. The evaluation involves analyzing scatter plots, convergence curves, coefficient comparison, and statistical metrics. The results depicted in Figs. 9 and 10, as well as Tables 6 and 7, provide insights into the superiority of the IARO algorithm compared to ARO and other existing approaches. Figs. 9(a) and 9(b) illustrate the scatter plots obtained for all 30 runs of the algorithms for the fourth-order system, considering reduced and same order IIR filters. These scatter plots exhibit a similar pattern to the previous cases of second and third-order systems (Figs. 5 and 7). Specifically, Fig. 9(a) demonstrates that the IARO algorithm consistently yields lower values compared to ARO. Similarly, in Fig. 9(b), the majority of data points obtained with IARO are lower than those obtained with ARO, indicating the algorithm's improved performance for both same order and reduced order IIR filters. Furthermore, Fig. 10 presents the convergence curves for the fourth-order system, considering the same order (Fig. 10(a)) and reduced order (Fig. 10(b)) IIR filters. Similar to the previous cases, the convergence curves demonstrate the progression of the algorithms over iterations. IARO achieves lower MSE values for both same order and reduced order cases, indicating its effectiveness in minimizing the error and converging to superior solutions.

Table 6 provides a detailed comparison of the coefficients obtained for the fourth-order system using the IARO and ARO algorithms. Analyzing the coefficients obtained with IARO reveals that they generally yield closer to the real values for most parameters compared to ARO. This indicates the IARO algorithm's ability to optimize the system coefficients effectively, leading to improved performance and accuracy. Table 7 reports the statistical values of different methods, including ARO [51], bat algorithm (BA) [55], Lévy flight trajectory-based whale optimization algorithm (LWOA) [55], grey wolf optimizer with ranking-based mutation operator (RGWO) [55], and dynamic opposite learning enhanced artificial ecosystem optimizer (DAEO) [55], for the fourth-order system modeled with reduced and same order IIR filters. The statistical metrics are evaluated separately for the same order and reduced order cases.

Analyzing Table 7, we observe that the IARO algorithm outperforms the other methods in terms of the best values across all metrics for both the same order and reduced order cases. IARO achieves significantly lower best values compared to ARO and the alternative methods, indicating its superior performance. Additionally, the algorithm demonstrates favorable results in terms of worst, mean, and standard deviation values, showcasing its robustness and stability in generating consistently better outcomes.

In summary, the evaluation of the fourth-order system reaffirms the superiority of the IARO algorithm over ARO and other existing approaches. The analysis of scatter plots, convergence curves, coefficient comparison, and statistical metrics consistently highlights the improved performance of IARO in terms of achieving lower MSE, better convergence, optimized coefficients, and superior statistical values. These findings establish the effectiveness and superiority of the IARO algorithm for the fourth-order system.

5.4. Fifth order system

In this section, we extend our analysis to a fifth-order system and evaluate the performance of the IARO algorithm. The assessment includes scatter plots, convergence curves, coefficient comparison, and statistical metrics. The results, illustrated in Figs. 11 and 12, as well as Tables 8 and 9, provide valuable insights into the effectiveness of the IARO algorithm for the considered fifth-order system.

Fig. 11 presents scatter plots obtained for all 30 runs of the algorithms, considering reduced and same order IIR filters for the fifth-order

Table 5
Reported statistical values of different methods for the third order system modeled with the same and reduced order IIR filters.

Type	Metric	IARO	ARO	CSO	FFA	HPSO-GSA	CSHO
Same order	Best	$\mathbf{9.8757 \times 10^{-32}}$	3.1658×10^{-16}	6.35201×10^{-5}	6.03×10^{-4}	1.55×10^{-3}	9.66×10^{-29}
	Worst	$\mathbf{1.4190 \times 10^{-25}}$	5.5955×10^{-11}	6.35201×10^{-5}	1.87×10^{-2}	9.20×10^{-3}	2.40×10^{-25}
	Mean	$\mathbf{2.0298 \times 10^{-26}}$	2.4660×10^{-12}	6.35201×10^{-5}	1.27×10^{-2}	5.43×10^{-3}	3.23×10^{-26}
	Standard Deviation	$\mathbf{3.3291 \times 10^{-26}}$	1.0267×10^{-11}	1.68717×10^{-18}	4.96×10^{-3}	2.13×10^{-3}	5.46×10^{-26}
Reduced order	Best	$\mathbf{5.1848 \times 10^{-4}}$	5.4238×10^{-4}	0.001393846	3.14×10^{-3}	1.53×10^{-3}	5.20×10^{-4}
	Worst	$\mathbf{6.0296 \times 10^{-4}}$	6.7935×10^{-4}	0.001393846	2.14×10^{-2}	8.05×10^{-3}	7.45×10^{-4}
	Mean	$\mathbf{5.7846 \times 10^{-4}}$	6.1436×10^{-4}	0.001393846	1.24×10^{-2}	3.94×10^{-3}	6.52×10^{-4}
	Standard Deviation	$\mathbf{2.3145 \times 10^{-5}}$	3.8365×10^{-5}	1.0842×10^{-19}	4.70×10^{-3}	1.61×10^{-3}	4.91×10^{-5}

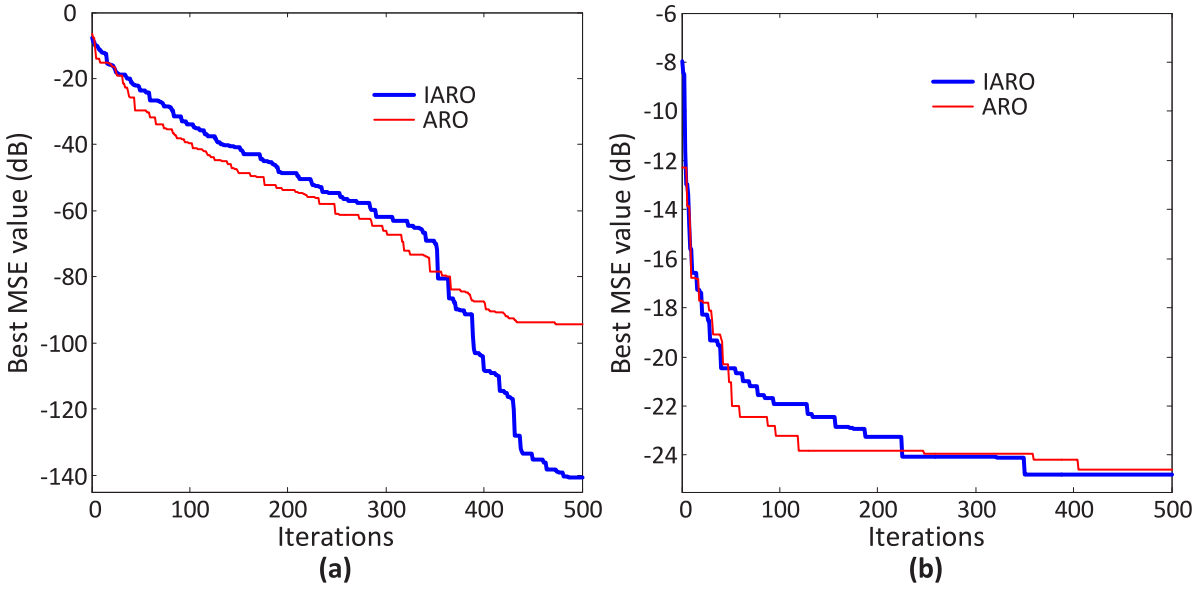


Fig. 10. Convergence curves obtained for fourth order system modeled with (a) same order and (b) reduced order IIR filters.

Table 6
The coefficients obtained for fourth order system.

Type	Coefficients	IARO	ARO
Same order	a_1	−0.040000592685006	−0.040032921481513
	a_2	−0.277500038362770	−0.277523395721592
	a_3	0.210100173789422	0.210049553077616
	a_4	−0.139999722985085	−0.140045467892456
	b_0	0.999999901046974	0.999976118469175
	b_1	−0.899999446607367	−0.899951536536422
	b_2	0.809999381423445	0.809964225776246
	b_3	−0.728999769621451	−0.728937583614310
Reduced order	a'_1	−0.921607029275574	−0.920081682764825
	a'_2	−0.747757460347637	−0.722676653094890
	a'_3	−0.098218859095828	−0.082581089702253
	b'_0	0.974795108953559	0.986047601161644
	b'_1	0.052616545573838	0.015019846725832
	b'_2	0.663473896344331	0.625149048753122

system. These scatter plots exhibit a similar pattern to the previously presented second, third, and fourth-order cases (Figs. 5, 7, and 9). Specifically, in Fig. 11(a), the majority of data points obtained through IARO are lower than those obtained through ARO, indicating the algorithm's ability to achieve better results. Similarly, Fig. 11(b) demonstrates that IARO consistently outperforms ARO in terms of achieving lower values for the majority of data points, reinforcing its superiority for both same order and reduced order IIR filters. Furthermore, Fig. 12 showcases the convergence curves for the fifth-order system, considering the same order (Fig. 12(a)) and reduced order (Fig. 12(b)) IIR filters. These curves track the progress of the algorithms over iterations. It is evident that IARO consistently achieves lower MSE values, surpassing the performance of ARO. This emphasizes the IARO algorithm's capability to minimize the error and converge to superior solutions for both the same order and reduced order cases.

Table 8 provides a detailed comparison of the coefficients obtained for the fifth-order system using the IARO and ARO algorithms. Analyzing the coefficients obtained with IARO reveals that they generally yield closer to the real values for most parameters compared to ARO. This signifies the IARO algorithm's effectiveness in optimizing the system coefficients, resulting in improved performance and accuracy for the fifth-order system. Table 9 reports the statistical values of different methods, including ARO [51], genetic algorithm (GA) [23], gravitational search algorithm (GSA) [23], inclined planes system optimization (IPO) [23], and particle swarm optimization (PSO) [23], for the fifth-order system modeled with reduced and same order IIR filters. The statistical metrics are assessed separately for the same order and reduced order cases.

Upon examining Table 9, it becomes apparent that the IARO algorithm consistently outperforms the other methods in terms of the best values for all metrics, both in the reduced and same order cases. The best values obtained through IARO are significantly lower compared to ARO and the alternative methods, showcasing its superior performance. Additionally, IARO demonstrates favorable results in terms of worst, mean, and standard deviation values, indicating its robustness and stability in consistently generating improved outcomes.

5.5. Non-parametric statistical test

In this section, we present the results of the non-parametric Wilcoxon signed-rank test conducted to assess the statistical significance of the performance differences between the proposed IARO and ARO algorithms for various IIR model types and orders. As indicated in Table 10,

Table 7
Reported statistical values of different methods for the fourth order system modeled with the same and reduced order IIR filters.

Type	Metric	IARO	ARO	BA	LWOA	RGWO	DAEO
Same order	Best	**8.4184×10^{-15}**	3.7232×10^{-10}	9.44×10^{-2}	1.48×10^{-3}	1.07×10^{-5}	2.17×10^{-11}
	Worst	**2.5921×10^{-11}**	1.8990×10^{-6}	1.41×10^{3}	4.48×10^{-2}	6.46×10^{-3}	9.91×10^{-4}
	Mean	**6.7930×10^{-12}**	2.9966×10^{-7}	4.97×10^{1}	1.28×10^{-2}	6.10×10^{-4}	7.91×10^{-5}
	Standard Deviation	**8.2847×10^{-12}**	5.2210×10^{-7}	2.56×10^{2}	1.06×10^{-2}	1.21×10^{-3}	2.12×10^{-4}
Reduced order	Best	3.3049×10^{-3}	3.4647×10^{-3}	4.32×10^{-2}	7.45×10^{-3}	3.70×10^{-3}	**2.65×10^{-3}**
	Worst	**3.7414×10^{-3}**	4.2868×10^{-3}	2.00	2.58×10^{-2}	1.08×10^{-2}	9.00×10^{-3}
	Mean	**3.6237×10^{-3}**	3.8932×10^{-3}	3.86×10^{-1}	1.59×10^{-2}	8.15×10^{-3}	4.12×10^{-3}
	Standard Deviation	**1.0285×10^{-4}**	2.0011×10^{-4}	3.95×10^{-1}	4.80×10^{-3}	2.83×10^{-3}	1.65×10^{-3}

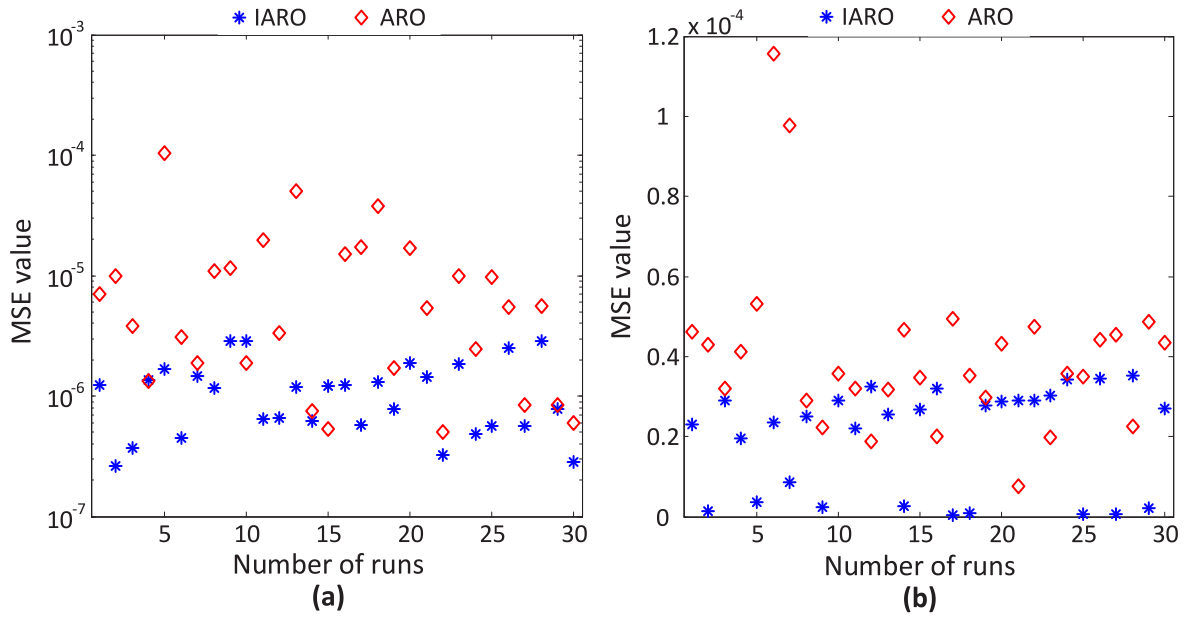


Fig. 11. Scatter plots obtained for all 30 runs of algorithms for fifth order system modeled with (a) same order and (b) reduced order IIR filters.

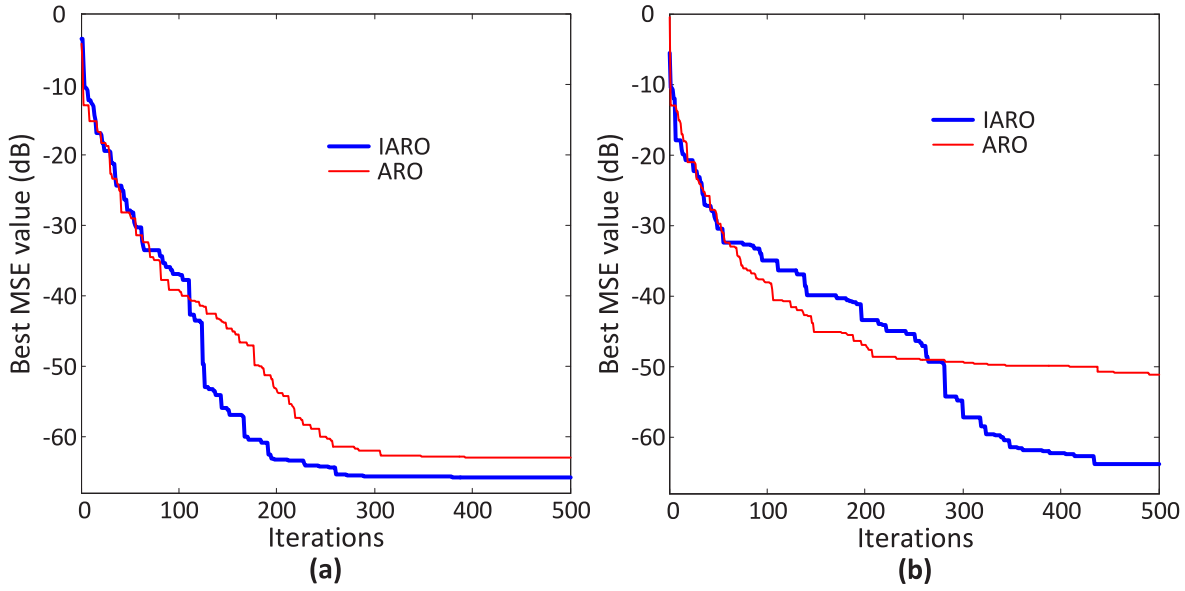


Fig. 12. Convergence curves obtained for fifth order system modeled with (a) same order and (b) reduced order IIR filters.

the Wilcoxon signed-rank test results consistently demonstrate that the proposed IARO algorithm outperforms the original ARO algorithm across different system types and model orders. The obtained p-values are remarkably small, all being less than the significance level of 0.05, indicating highly significant differences in performance. In each case, IARO is identified as the winner, signifying its superior effectiveness in optimizing system parameters and achieving lower MSE values. These statistical findings further validate the efficacy of the IARO algorithm in consistently generating solutions with superior performance and accuracy for various IIR system identification scenarios. The consistent

Table 8
The coefficients obtained for fifth order system.

Type	Coefficients	IARO	ARO
Same order	a_1	−0.091963933310944	0.065510253050007
	a_2	−0.417953338036308	−0.307012318191027
	a_3	0.231718561869757	0.339737837716779
	a_4	−0.000226928316145	0.026777962496099
	a_5	0.023273128348011	0.027060252938902
	b_0	0.108415440623010	0.108459219572242
	b_1	0.445050812699318	0.427785083238135
	b_2	0.634505033342557	0.554729983368939
	b_3	0.283668284692613	0.137213599490555
	b_4	−0.113062384689373	−0.235594502183365
	b_5	−0.103891170657143	−0.144786499761215
Reduced order	a'_1	−0.577526454538850	−0.363079459305462
	a'_2	−0.688559929527913	−0.660369905501358
	a'_3	−0.101214412003194	0.005132125362190
	a'_4	−0.044934419547747	−0.065475146761729
	b'_0	0.107788331761506	0.107446027740990
	b'_1	0.497356787857328	0.473489256729425
	b'_2	0.874769314421812	0.781468233723383
	b'_3	0.704424827667655	0.562972141905722
	b'_4	0.222506867289702	0.143292293426391

superiority of IARO, as evidenced by the statistical analysis with p-values less than 0.05, reinforces its potential as a valuable tool for researchers and practitioners in the field of signal processing and system identification.

5.6. Discussion

The previous subsections presented a comprehensive analysis of the proposed IARO algorithm for IIR system identification. The evaluation encompassed different orders of IIR systems, including second, third, fourth, and fifth order. In this section, we discuss the results obtained and provide a comprehensive understanding of the efficacy of the IARO algorithm. The results consistently demonstrate that the IARO algorithm outperforms the conventional ARO algorithm in terms of system identification accuracy and convergence. Across all orders of IIR systems, IARO consistently achieves lower mean square error (MSE) values, indicating its superior ability to minimize the discrepancy between the estimated and actual system outputs.

In terms of scatter plots, the visual analysis reveals a distinct pattern. For all orders of IIR systems, IARO consistently generates data points that are predominantly lower than those obtained through ARO. This observation suggests that the IARO algorithm is effective in finding optimal solutions that closely match the actual system behavior. The convergence curves further confirm this trend, as IARO consistently converges to lower MSE values compared to ARO. The superior convergence characteristics of IARO indicate its ability to explore the search space efficiently and identify optimal solutions.

The analysis of coefficient comparison supports the efficacy of the IARO algorithm in optimizing the system parameters. In all cases, the coefficients obtained through IARO tend to be closer to the real values compared to ARO. This implies that the IARO algorithm is able to fine-tune the system parameters more effectively, resulting in improved system identification accuracy. Furthermore, the comparison of statistical metrics validates the superiority of the IARO algorithm. Across all orders of IIR systems, IARO consistently achieves the best values for the metrics, including best, worst, mean, and standard deviation. The best values obtained through IARO are significantly lower than those obtained through ARO and other alternative methods. This indicates the IARO algorithm's ability to consistently generate solutions with superior performance and accuracy.

The inclusion of the Wilcoxon signed-rank test results reinforces our discussion by providing statistical evidence for the observed performance differences between IARO and ARO. All obtained p-values are remarkably small, all being less than the significance level of 0.05, indicating highly significant differences in performance. In each case, IARO emerges as the winner, confirming its superiority in optimizing system parameters and achieving lower MSE values.

Overall, the comprehensive analysis of the IARO algorithm for IIR system identification reveals its efficacy and superiority over the conventional ARO algorithm. The algorithm consistently achieves lower MSE values, better convergence, optimized system coefficients, and superior statistical metrics. These findings highlight the IARO algorithm's ability to effectively explore the search space, identify optimal solutions, and accurately model the underlying IIR systems. Accurate modeling of IIR systems is crucial in various domains, including signal processing, control systems, and communication systems. The IARO algorithm's ability to achieve higher accuracy and convergence offers practical advantages in optimizing system performance, enabling more precise control and efficient utilization of resources. In conclusion, the evaluation of the IARO algorithm for IIR system identification across multiple orders of IIR systems highlights its efficacy and superiority over the conventional ARO algorithm. The algorithm consistently achieves lower MSE values, better convergence, optimized system coefficients, and superior statistical metrics. These findings demonstrate the IARO algorithm's ability to accurately model and identify IIR systems, making it a valuable tool in various domains requiring precise system characterization and control.

6. Conclusion

In this paper, we have proposed an improved version of the ARO algorithm called IARO for the identification of models with IIR. The IARO algorithm addresses the limitations of ARO by incorporating an adaptive local search mechanism and an experience-based perturbed learning strategy. Through comprehensive empirical evaluation and performance analysis, we have demonstrated the superior effectiveness and efficiency of IARO in identifying IIR systems. The results of our experiments consistently indicate that the IARO algorithm surpasses the conventional ARO algorithm in terms of accuracy and convergence for system identification across different orders of IIR systems. The IARO algorithm consistently achieves lower MSE values, indicating its ability to minimize the discrepancy between estimated and actual system outputs. Visual analysis of scatter plots reveals that IARO generates data points predominantly lower than those obtained through ARO,

Table 9
Reported statistical values of different methods for the fifth order system modeled with the same and reduced order IIR filters.

Type	Metric	IARO	ARO	GA	GSA	IPO	PSO
Same order	Best	$\mathbf{2.6342 \times 10^{-7}}$	5.0354×10^{-7}	8.8033×10^{-5}	4.8656×10^{-5}	4.8542×10^{-5}	5.1985×10^{-5}
	Worst	$\mathbf{2.8831 \times 10^{-6}}$	1.0416×10^{-4}	8.8033×10^{-5}	9.8739×10^{-5}	8.1884×10^{-5}	9.8948×10^{-5}
	Mean	$\mathbf{1.1806 \times 10^{-6}}$	1.2019×10^{-5}	8.8033×10^{-5}	7.7387×10^{-5}	6.5836×10^{-5}	8.0999×10^{-5}
	Standard Deviation	7.8643×10^{-7}	2.0706×10^{-5}	**0**	1.8004×10^{-5}	1.1977×10^{-5}	1.6851×10^{-5}
Reduced order	Best	$\mathbf{4.0842 \times 10^{-7}}$	7.6693×10^{-6}	9.0526×10^{-5}	4.7195×10^{-5}	5.8187×10^{-5}	6.0534×10^{-5}
	Worst	$\mathbf{3.5162 \times 10^{-5}}$	1.1572×10^{-4}	0.00028314	0.00024126	0.00012361	0.00010584
	Mean	$\mathbf{1.9556 \times 10^{-5}}$	4.0264×10^{-5}	0.00015238	8.1244×10^{-5}	8.2263×10^{-5}	8.2009×10^{-5}
	Standard Deviation	$\mathbf{1.2967 \times 10^{-5}}$	2.1237×10^{-5}	6.7789×10^{-5}	4.3547×10^{-5}	1.5695×10^{-5}	1.7583×10^{-5}

Table 10
Wilcoxon signed-rank test between proposed IARO and ARO.

System type		p-value	Winner
Second order	Same order model	1.7344×10^{-6}	IARO
	Reduced order model	3.1108×10^{-5}	IARO
Third order	Same order model	1.7344×10^{-6}	IARO
	Reduced order model	6.6392×10^{-4}	IARO
Fourth order	Same order model	1.7344×10^{-6}	IARO
	Reduced order model	6.3391×10^{-6}	IARO
Fifth order	Same order model	1.1265×10^{-5}	IARO
	Reduced order model	5.2872×10^{-4}	IARO

suggesting its effectiveness in finding optimal solutions that closely match the actual system behavior. Convergence curves further confirm this trend, as IARO consistently converges to lower MSE values compared to ARO, demonstrating its superior ability to explore the search space efficiently and identify optimal solutions. The analysis of coefficient comparison supports the effectiveness of the IARO algorithm in optimizing system parameters. The coefficients obtained through IARO exhibit closer values to the real ones compared to ARO, indicating its superior ability to fine-tune system parameters and improve system identification accuracy. Statistical metrics comparison validates the superiority of the IARO algorithm, with IARO consistently achieving the best values for metrics such as best, worst, mean, and standard deviation. The superiority of IARO is evident as it consistently outperforms ARO and other alternative methods, generating solutions with superior performance and accuracy. Additionally, the Wilcoxon signed-rank test results provide further statistical evidence supporting the superior performance of IARO. In summary, the comprehensive analysis of the IARO algorithm for IIR system identification demonstrates its efficacy and superiority over the conventional ARO algorithm and other existing methods. The IARO algorithm effectively explores the search space, identifies optimal solutions, and accurately models underlying IIR systems. It represents a significant advancement in the pursuit of superior effectiveness in IIR system identification. The proposed IARO algorithm offers a promising solution to the challenges of IIR model identification, overcoming the limitations of existing techniques such as slow convergence, sensitivity to initial conditions, and suboptimal performance. By integrating an adaptive local search mechanism and an experience-based perturbed learning strategy, IARO strikes a balance between exploration and exploitation, improving solution diversity and navigating towards promising regions during the iterative search. These advancements contribute to the accurate and efficient identification of IIR systems, enabling better design and optimization of systems relying on them. Future research can focus on further enhancing the IARO algorithm and exploring its applicability to other challenging problems in signal processing and system identification. Additionally, investigating the integration of IARO with other optimization techniques or hybrid approaches could potentially yield even more powerful and efficient methods for addressing IIR system identification challenges.

Ethical approval

This article does not contain any studies with human participants or animals performed by any of the authors.

Informed consent

Informed consent was obtained from all individual participants included in the study.

Declaration of competing interest

The authors declare that they have no known competing financial interests or personal relationships that could have appeared to influence the work reported in this paper.

Data availability

No data was used for the research described in the article.

References

[1] W. Zhu, J. Fang, Y. Tang, W. Zhang, W. Du, Digital IIR filters design using differential evolution algorithm with a controllable probabilistic population size, PLoS One 7 (2012) e40549, http://dx.doi.org/10.1371/journal.pone.0040549.

[2] D. Izci, S. Ekinci, M. Güleydin, Application of slime mould algorithm to infinite impulse response system identification problem, Comput. Sci. IDAP-2022 (2022) 45–51, http://dx.doi.org/10.53070/bbd.1172833.

[3] F. Alenezi, RGB-based triple-dual-path recurrent network for underwater image dehazing, Electronics (Basel) 11 (2022) 2894, http://dx.doi.org/10.3390/electronics11182894.

[4] G.S. Nikolić, T.R. Nikolić, G.Lj. Djordjević, Adaptive control based on LMS algorithm for grid-connected inverters, Electr. Power Compon. Syst. 51 (2023) 656–668, http://dx.doi.org/10.1080/15325008.2023.2180815.

[5] A. Kumar, N. Agrawal, I. Sharma, Design of Finite Impulse Response Filter with Controlled Ripple using Cuckoo Search Algorithm, 2020, pp. 471–482, http://dx.doi.org/10.1007/978-981-32-9291-8_37.

[6] M. Zelmat, E.-S. Lamini, S. Tagzout, H. Belbachir, A. Belouchrani, Multi-objective approach for IIR filter design and bit-width optimization, Circuits Systems Signal Process. (2023) http://dx.doi.org/10.1007/s00034-023-02334-1.

[7] N. Agrawal, A. Kumar, V. Bajaj, G.K. Singh, Design of digital IIR filter: A research survey, Appl. Acoust. 172 (2021) 107669, http://dx.doi.org/10.1016/j.apacoust.2020.107669.

[8] S.K. Saha, R. Kar, D. Mandal, S.P. Ghoshal, Harmony search algorithm for infinite impulse response system identification, Comput. Electr. Eng. 40 (2014) 1265–1285, http://dx.doi.org/10.1016/j.compeleceng.2013.12.016.

[9] S. Jiang, Y. Wang, Z. Ji, A new design method for adaptive IIR system identification using hybrid particle swarm optimization and gravitational search algorithm, Nonlinear Dyn. 79 (2015) 2553–2576, http://dx.doi.org/10.1007/s11071-014-1832-0.

[10] D. Iannuzzi, M. Ribera, P. Satariano, E. Fedele, F. Pagliarini, P. Cennamo, F. Orsini, L. Petrazzuoli, M. Spinelli, Capacity fade estimation of LiFePo cells based on improved impulse response method: Experimental results, in: 2023 IEEE International Conference on Electrical Systems for Aircraft, Railway, Ship Propulsion and Road Vehicles & International Transportation Electrification Conference, ESARS-ITEC, IEEE, 2023, pp. 1–6, http://dx.doi.org/10.1109/ESARS-ITEC57127.2023.10114873.

[11] S. Choi, Identifying parametric models used to estimate track irregularities of a high-speed railway, Machines 11 (2022) 6, http://dx.doi.org/10.3390/machines11010006.

[12] E. Cuevas, O. Avalos, J. Gálvez, IIR System Identification using Several Optimization Techniques: A Review Analysis, 2023, pp. 89–104, http://dx.doi.org/10.1007/978-3-031-20105-9_5.

[13] N. Agrawal, A. Kumar, V. Bajaj, A new design method for stable IIR filters with nearly linear-phase response based on fractional derivative and swarm intelligence, IEEE Trans. Emerg. Top Comput. Intell. 1 (2017) 464–477, http://dx.doi.org/10.1109/TETCI.2017.2748151.

[14] A. Kumar, N. Agrawal, I. Sharma, S. Lee, H.-N. Lee, Hilbert transform design based on fractional derivatives and swarm optimization, IEEE Trans. Cybern. 50 (2020) 2311–2320, http://dx.doi.org/10.1109/TCYB.2018.2875540.

[15] N. Agrawal, A. Kumar, V. Bajaj, G.K. Singh, Design of bandpass and bandstop infinite impulse response filters using fractional derivative, IEEE Trans. Ind. Electron. 66 (2019) 1285–1295, http://dx.doi.org/10.1109/TIE.2018.2831184.

[16] S.K. Saha, R. Kar, D. Mandal, S.P. Ghoshal, Design and simulation of FIR band pass and band stop filters using gravitational search algorithm, Memet. Comput. 5 (2013) 311–321, http://dx.doi.org/10.1007/s12293-013-0122-6.

[17] K.M. Ong, P. Ong, C.K. Sia, A new flower pollination algorithm with improved convergence and its application to engineering optimization, Decis. Anal. J. 5 (2022) 100144, http://dx.doi.org/10.1016/j.dajour.2022.100144.

[18] M.S. Shaikh, S. Raj, R. Babu, S. Kumar, K. Sagrolikar, A hybrid moth–flame algorithm with particle swarm optimization with application in power transmission and distribution, Decis. Anal. J. 6 (2023) 100182, http://dx.doi.org/10.1016/j.dajour.2023.100182.

[19] M. Ghasemi, S. kadkhoda Mohammadi, M. Zare, S. Mirjalili, M. Gil, R. Hemmati, A new firefly algorithm with improved global exploration and convergence with application to engineering optimization, Decis. Anal. J. 5 (2022) 100125, http://dx.doi.org/10.1016/j.dajour.2022.100125.

[20] M. Zare, M.-A. Akbari, R. Azizipanah-Abarghooee, M. Malekpour, S. Mirjalili, L. Abualigah, A modified Particle Swarm Optimization algorithm with enhanced search quality and population using Hummingbird Flight patterns, Decis. Anal. J. 7 (2023) 100251, http://dx.doi.org/10.1016/j.dajour.2023.100251.

[21] M. Azizi, S. Talatahari, M. Basiri, M. Baghalzadeh Shishehgarkhaneh, Optimal design of low- and high-rise building structures by Tribe-Harmony Search

algorithm, Decis. Anal. J. 3 (2022) 100067, http://dx.doi.org/10.1016/j.dajour.2022.100067.
[22] A. Banharnsakun, A new approach for solving the minimum vertex cover problem using artificial bee colony algorithm, Decis. Anal. J. 6 (2023) 100175, http://dx.doi.org/10.1016/j.dajour.2023.100175.
[23] A. Mohammadi, S.H. Zahiri, S.M. Razavi, Infinite impulse response systems modeling by artificial intelligent optimization methods, Evol. Syst. 10 (2019) 221–237, http://dx.doi.org/10.1007/s12530-018-9218-z.
[24] J. Zhang, G. Zhang, M. Kong, T. Zhang, Adaptive infinite impulse response system identification using an enhanced golden jackal optimization, J. Supercomput. 79 (2023) 10823–10848, http://dx.doi.org/10.1007/s11227-023-05086-6.
[25] X. Liang, Z. Zhang, A whale optimization algorithm with convergence and exploitability enhancement and its application, Math. Probl. Eng. 2022 (2022) 1–19, http://dx.doi.org/10.1155/2022/2904625.
[26] Q. Luo, Y. Ling, Y. Zhou, Modified whale optimization algorithm for infinitive impulse response system identification, Arab. J. Sci. Eng. 45 (2020) 2163–2176, http://dx.doi.org/10.1007/s13369-019-04093-1.
[27] B. Durmuş, Infinite impulse response system identification using average differential evolution algorithm with local search, Neural Comput. Appl. 34 (2022) 375–390, http://dx.doi.org/10.1007/s00521-021-06399-4.
[28] N. Agrawal, A. Kumar, V. Bajaj, Digital IIR filter design with controlled ripple using cuckoo search algorithm, in: 2016 International Conference on Signal and Information Processing, IConSIP, IEEE, 2016, pp. 1–5, http://dx.doi.org/10.1109/ICONSIP.2016.7857464.
[29] S. Ansari, G. Kishor, P.K. Verma, N. Agrawal, I. Sharma, A. Kumar, Design of multiplierless digital IIR filter using modified cuckoo search algorithm, in: 2018 International Conference on Communication and Signal Processing, ICCSP, IEEE, 2018, pp. 0405–0410, http://dx.doi.org/10.1109/ICCSP.2018.8524139.
[30] M. Kaur, R. Kaur, N. Singh, A novel hybrid of chimp with cuckoo search algorithm for the optimal designing of digital infinite impulse response filter using high-level synthesis, Soft Comput. 26 (2022) 13843–13867, http://dx.doi.org/10.1007/s00500-022-07410-3.
[31] A. Liu, P. Li, X. Deng, L. Ren, A sigmoid attractiveness based improved firefly algorithm and its applications in IIR filter design, Connect. Sci. 33 (2021) 1–25, http://dx.doi.org/10.1080/09540091.2020.1742660.
[32] X. Liang, D. Wu, Y. Liu, M. He, L. Sun, An enhanced slime mould algorithm and its application for digital IIR filter design, Discrete Dyn. Nat. Soc. 2021 (2021) 1–23, http://dx.doi.org/10.1155/2021/5333278.
[33] S. Singh, A. Ashok, M. Kumar, T.K. Rawat, Adaptive infinite impulse response system identification using teacher learner based optimization algorithm, Appl. Intell. 49 (2019) 1785–1802, http://dx.doi.org/10.1007/s10489-018-1354-4.
[34] S. Zhang, Y. Zhou, Grey wolf optimizer with ranking-based mutation operator for IIR model identification, Chin. J. Electron. 27 (2018) 1071–1079, http://dx.doi.org/10.1049/cje.2018.06.008.
[35] M. Kumar, T.K. Rawat, A. Aggarwal, Adaptive infinite impulse response system identification using modified-interior search algorithm with Lèvy flight, ISA Trans. 67 (2017) 266–279, http://dx.doi.org/10.1016/j.isatra.2016.10.018.
[36] P. Upadhyay, R. Kar, D. Mandal, S.P. Ghoshal, A new design method based on firefly algorithm for IIR system identification problem, J. King Saud Univ., Eng. Sci. 28 (2016) 174–198, http://dx.doi.org/10.1016/j.jksues.2014.03.001.
[37] P. Lagos-Eulogio, J.C. Seck-Tuoh-Mora, N. Hernandez-Romero, J. Medina-Marin, A new design method for adaptive IIR system identification using hybrid CPSO and DE, Nonlinear Dyn. 88 (2017) 2371–2389, http://dx.doi.org/10.1007/s11071-017-3383-7.
[38] S.P. Ghoshal, S.K. Saha, R. Kar, D. Mandal, Seeker optimisation algorithm: application to the design of linear phase finite impulse response filter, IET Signal Process. 6 (2012) 763–771, http://dx.doi.org/10.1049/iet-spr.2011.0353.
[39] N. Agrawal, A. Kumar, V. Bajaj, Optimized design of digital IIR filter using artificial bee colony algorithm, in: 2015 International Conference on Signal Processing, Computing and Control, ISPCC, IEEE, 2015, pp. 316–321, http://dx.doi.org/10.1109/ISPCC.2015.7375048.
[40] N. Agrawal, A. Kumar, V. Bajaj, Design of digital IIR filter with low quantization error using hybrid optimization technique, Soft Comput. 22 (2018) 2953–2971, http://dx.doi.org/10.1007/s00500-017-2548-0.
[41] N. Agrawal, A. Kumar, V. Bajaj, Design of infinite impulse response filter using fractional derivative constraints and hybrid particle swarm optimization, Circuits Systems Signal Process. 39 (2020) 6162–6190, http://dx.doi.org/10.1007/s00034-020-01456-0.
[42] N. Agrawal, A. Kumar, V. Bajaj, A new method for designing of stable digital IIR filter using hybrid method, Circuits Systems Signal Process. 38 (2019) 2187–2226, http://dx.doi.org/10.1007/s00034-018-0959-5.
[43] Chaohua Dai, Weirong Chen, Yunfang Zhu, Seeker optimization algorithm for digital IIR filter design, IEEE Trans. Ind. Electron. 57 (2010) 1710–1718, http://dx.doi.org/10.1109/TIE.2009.2031194.
[44] B. Luitel, G.K. Venayagamoorthy, Particle swarm optimization with quantum infusion for system identification, Eng. Appl. Artif. Intell. 23 (2010) 635–649, http://dx.doi.org/10.1016/j.engappai.2010.01.022.
[45] R.M. Rizk-Allah, A.A. El-Fergany, E.A. Gouda, M.F. Kotb, Characterization of electrical 1-phase transformer parameters with guaranteed hotspot temperature and aging using an improved dwarf mongoose optimizer, Neural Comput. Appl. 35 (2023) 13983–13998, http://dx.doi.org/10.1007/s00521-023-08449-5.
[46] R.M. Rizk-Allah, A.A. El-Fergany, Conscious neighborhood scheme-based Laplacian barnacles mating algorithm for parameters optimization of photovoltaic single- and double-diode models, Energy Convers. Manag. 226 (2020) 113522, http://dx.doi.org/10.1016/j.enconman.2020.113522.
[47] V. Snášel, R.M. Rizk-Allah, D. Izci, S. Ekinci, Weighted mean of vectors optimization algorithm and its application in designing the power system stabilizer, Appl Soft Comput. 136 (2023) 110085, http://dx.doi.org/10.1016/j.asoc.2023.110085.
[48] H. Garg, R.M. Rizk-Allah, A novel approach for solving rough multi-objective transportation problem: development and prospects, Comput. Appl. Math. 40 (2021) 149, http://dx.doi.org/10.1007/s40314-021-01507-5.
[49] R.M. Rizk-Allah, A.A. El-Fergany, Effective coordination settings for directional overcurrent relay using hybrid gradient-based optimizer, Appl Soft Comput. 112 (2021) 107748, http://dx.doi.org/10.1016/j.asoc.2021.107748.
[50] R.M. Rizk-Allah, A quantum-based sine cosine algorithm for solving general systems of nonlinear equations, Artif. Intell. Rev. 54 (2021) 3939–3990, http://dx.doi.org/10.1007/s10462-020-09944-0.
[51] L. Wang, Q. Cao, Z. Zhang, S. Mirjalili, W. Zhao, Artificial rabbits optimization: A new bio-inspired meta-heuristic algorithm for solving engineering optimization problems, Eng. Appl. Artif. Intell. 114 (2022) 105082, http://dx.doi.org/10.1016/j.engappai.2022.105082.
[52] Y. Yang, B. Yang, M. Niu, Adaptive infinite impulse response system identification using opposition based hybrid coral reefs optimization algorithm, Appl. Intell. 48 (2018) 1689–1706, http://dx.doi.org/10.1007/s10489-017-1034-9.
[53] G. Panda, P.M. Pradhan, B. Majhi, IIR system identification using cat swarm optimization, Expert Syst. Appl. 38 (2011) 12671–12683, http://dx.doi.org/10.1016/j.eswa.2011.04.054.
[54] R. Zhao, Y. Wang, C. Liu, P. Hu, H. Jelodar, C. Yuan, Y. Li, I. Masood, M. Rabbani, H. Li, B. Li, Selfish herd optimization algorithm based on chaotic strategy for adaptive IIR system identification problem, Soft Comput. 24 (2020) 7637–7684, http://dx.doi.org/10.1007/s00500-019-04390-9.
[55] Y. Niu, X. Yan, Y. Wang, Y. Niu, Dynamic opposite learning enhanced artificial ecosystem optimizer for IIR system identification, J. Supercomput. 78 (2022) 13040–13085, http://dx.doi.org/10.1007/s11227-022-04367-w.
[56] N. Karaboga, A new design method based on artificial bee colony algorithm for digital IIR filters, J. Franklin Inst. 346 (2009) 328–348, http://dx.doi.org/10.1016/j.jfranklin.2008.11.003.
[57] N. Karaboga, Digital IIR filter design using differential evolution algorithm, EURASIP J. Adv. Signal Process. 2005 (2005) 856824, http://dx.doi.org/10.1155/ASP.2005.1269.
[58] S. Ekinci, D. Izci, Enhancing IIR system identification: Harnessing the synergy of gazelle optimization and simulated annealing algorithms, E-Prime - Adv. Electric. Eng. Electron. Energy 5 (2023) 100225, http://dx.doi.org/10.1016/j.prime.2023.100225.
[59] S. Ekinci, D. Izci, M. Yilmaz, Simulated annealing aided artificial hummingbird optimizer for infinite impulse response system identification, IEEE Access 11 (2023) 88627–88636, http://dx.doi.org/10.1109/ACCESS.2023.3303328.